

## Article

# The Correlation between Proximal and Remote Sensing Methods for Monitoring Soil Water Content in Agricultural Applications

Elio Romano <sup>1</sup>, Simone Bergonzoli <sup>2</sup>, Carlo Bisaglia <sup>1</sup>, Rodolfo Picchio <sup>3,\*</sup> and Antonio Scarfone <sup>2</sup>

<sup>1</sup> Council for Agricultural Research and Economics, Research Centre for Engineering and Agro-Food Processing, 24047 Treviglio, Italy

<sup>2</sup> Council for Agricultural Research and Economics, Research Centre for Engineering and Agro-Food Processing, 00015 Monterotondo, Italy

<sup>3</sup> Department of Agriculture and Forest Sciences (DAFNE), Tuscia University, 01100 Viterbo, Italy

\* Correspondence: r.picchio@unitus.it

**Abstract:** Water shortages have increasingly become a global issue due to the acceleration of climate change. The consumption of freshwater can be reduced to a minimum using water irrigation techniques that are based on conservative methods. For example, one of these is precision irrigation, or PI, which uses advanced digital technology to regulate the amount of water used. The aim is to use the least amount of water necessary for a given purpose. This approach keeps consumption to a minimum while the amount remains effective for its purpose. It is also important to note that the variability which occurs in soil and crops will create different types of conditions. These different conditions will need to be studied so as to determine the correct and adequate dynamics for a water management approach that is efficient. In this study, three investigation methods were developed and compared. The first evaluation was performed on outputs from the geoelectric reading of Automatic Resistivity Profiling (ARP). A second evaluation was performed in real time via a sensor network placed in the soil for the duration of two growing seasons of two different crops. The last evaluation was carried out by using maps of spectral indices obtained by the Sentinel 2 satellites. The correlations between the three methods were evaluated to verify if satellite information may have significant potential in the use of water management in varying conditions. From the results obtained, some correlations have been found from the observations of the three systems under study. This has given a positive input towards using satellite maps which are integrated with simplified proximal sensor networks. The outcome of this technique can improve the efficiency of how to manage water distribution on cultivated land.

**Keywords:** water management; irrigation techniques; variability; crop requirements; satellite maps



**Citation:** Romano, E.; Bergonzoli, S.; Bisaglia, C.; Picchio, R.; Scarfone, A. The Correlation between Proximal and Remote Sensing Methods for Monitoring Soil Water Content in Agricultural Applications. *Electronics* **2023**, *12*, 127. <https://doi.org/10.3390/electronics12010127>

Academic Editor: Amir Mosavi

Received: 16 November 2022

Revised: 20 December 2022

Accepted: 25 December 2022

Published: 28 December 2022



**Copyright:** © 2022 by the authors. Licensee MDPI, Basel, Switzerland. This article is an open access article distributed under the terms and conditions of the Creative Commons Attribution (CC BY) license (<https://creativecommons.org/licenses/by/4.0/>).

## 1. Introduction

Water shortage has become a serious issue on a global scale as a consequence of ongoing climate change. The growing number of extreme events such as heat waves, drought, violent storms, tornadoes, and hailstorms creates a situation of climatic chaos that often leads to environmental conditions which are above the tolerability level for many species of plants and animals, including human beings. In Italy, as in many other parts of the world, the mean annual temperature increases every year while precipitation decreases. An analysis carried out by the Italian National Institute for Environmental Protection and Research [1] based on the historical comparison of temperatures for the last 30 years showed that in this country, the temperature had risen by 0.035 °C every year. It corresponds to about half of the global average, which is over 0.08 °C since 1880 [2].

A comparison of the averages on rainfall for the period 2000–2009 shows that the average annual precipitation in Italy was 763 mm, which is 30 mm less than the average for

the years 1971 to 2000 [3]. The 2010–2020 decade was dramatic for Italy, with cumulative annual precipitations lower than 10% as compared to the mean of the previous decade, with peaks of drought that were much higher in southern Italy [4]. Another problem that Italy is now dealing with is rainfall fluctuation and intensity. The prolonged periods of drought, especially during the summer, have made these commonplace problems. The cause of these problems occurs when a large amount of water falls onto the soil in a short amount of time. The limited water retention capacity of the soil will allow the water to run off. Thus, there are water losses and other related problems such as soil erosion, increased risk of landslides, and flooding.

Agriculture is the sector that is the most demanding for water. Water consumption for agricultural purposes makes up about 70 percent of the total annual withdrawal of fresh water [5]. In extensive agriculture, water is distributed mostly by sprinkler irrigation and surface irrigation [6]. In sprinkler irrigation, the percentage of water loss can be up to 45% due to evaporation and other factors [7], while surface irrigation is even more wasteful, with losses that are about 35% higher than sprinkler irrigation [8]. These systems are not sustainable and should be improved or replaced so as to lessen the pressure of demand on the global fresh-water reservoirs. In recent years, the problem of water availability has seriously affected industrialized countries. The development of systems that are made to plan irrigation cycles and eliminate water loss is urgently needed.

Some advancement in technological development has been accomplished in this direction. For instance, precision irrigation applies water in minimal amounts and exclusively in the specified place at a predetermined time to create the best growing conditions for plants [9]. The precision irrigation system is based on soil sensors. These sensors are geo-localized and monitor the soil water content at different soil depths, providing remote information, and notifying or directly commanding the start of irrigation only where and when it is required [10–14]. There are several pros and cons to these systems. The pros include reliability, continuous monitoring, and precision. In contrast, the cons are the costs, the risks of damage during field operations, and the practical management [15]. For these last reasons, the installation of a dense sensor network in the field is not always feasible. Given the current levels of satellite images [16], the use of satellite imaging in combination with an on-site monitoring system is under study in both marine and terrestrial environments [17,18].

A review by Massari et al. (2021) [19] compiles about 50 scientific papers on using space technology for the retrieval of information for irrigation. The techniques consisted of visible and near-infrared sensors (VIS/NIR), microwave (MW), land surface models (LSM), and energy balance models (EBM). The authors gave observations about the advantages and disadvantages of each technique and concluded that the levels of action are very different, as are the capabilities of different satellite installations.

In a study conducted in the USA, De Lara et al. (2019) [20] studied soil water content (SWC) behavior by integrating information obtained from soil sensors by the Rapid Eye satellite constellation to determine the optimal time and depth of SWC and its relationship to maize grain yield. The study concluded that different sources of information could be combined to obtain more accurate models of soil water content and maize yield at the field level for precision irrigation.

In another study performed in Southeastern Canada by Ihuoma et al. (2020) [21], the suitability of multispectral images acquired from Unmanned Aerial Vehicles (UAV-MSI) and Sentinel-2A & 2B satellite platforms was compared with in-situ soil moisture data to estimate irrigation water requirements of field grown tomato crops (*Lycopersicon esculentum*). The researchers stressed the validity of this near real-time approach for supporting precision irrigation and preventing over-irrigation.

In any case, the precise determination of the rate of water application by the remote sensing approach requires further study. This is due to the high number of variables in cultivated lands. Soil water retention capacity and water plant requirements vary according to soil type, climate, plant species, and other site-specific factors. A challenging aspect

of soil water content detection using satellite technology is related to the condition of no vegetation. In fact, several of the cited scientific papers use satellite systems in the condition of soil vegetation, while no relevant approaches were identified for the condition of bare soils. Knowing the soil water content in the condition of bare ground can be very useful, especially for the success of seed emergence [22,23]. In this study, three investigation methods for monitoring soil water content were compared in Northern Italy in the Po valley. Two systems are based on proximal sensing and one on remote sensing, based on maps of spectral indices obtained by the Sentinel 2 satellites (A and B). The study aimed to evaluate the correlation between the three investigation techniques and highlight if satellite data obtained from remote sensing may have a high potential for use in water resource management and in no-vegetation conditions. The aim of the study is to determine if satellites are suitable for planning PI in the conditions that are found in Northern Italy.

## 2. Materials and Methods

The experimental tests were carried out in a portion of agricultural land located at the CREA-IT farm (Figure 1—yellow quadrilateral) in Treviglio, Bergamo, Northern Italy ( $45^{\circ}31'14''$  N;  $9^{\circ}35'27''$  E; +128 m a.s.l.). This 3.0 ha field is normally cultivated with the typical crop rotation: triticale for winter cultivation (*Triticosecale Wittmack*) and corn for spring-summer cultivation (*Zea mays*). According to the World Reference Base for Soil Resources [24], the soil was classified as Calcic Skeletic Mollic Umbrisol, with neutral-sub-alkaline pH and with the presence of carbonates on the surface. The period of observation started in July 2020, when corn was present, and concluded in April 2021, when triticale was present. No crops were present between 15 September and 10 November. However, the condition of uncultivated soil must be considered until 31 December since the emergence of triticale plants still represented a negligible percentage compared to the visible surface of the soil.

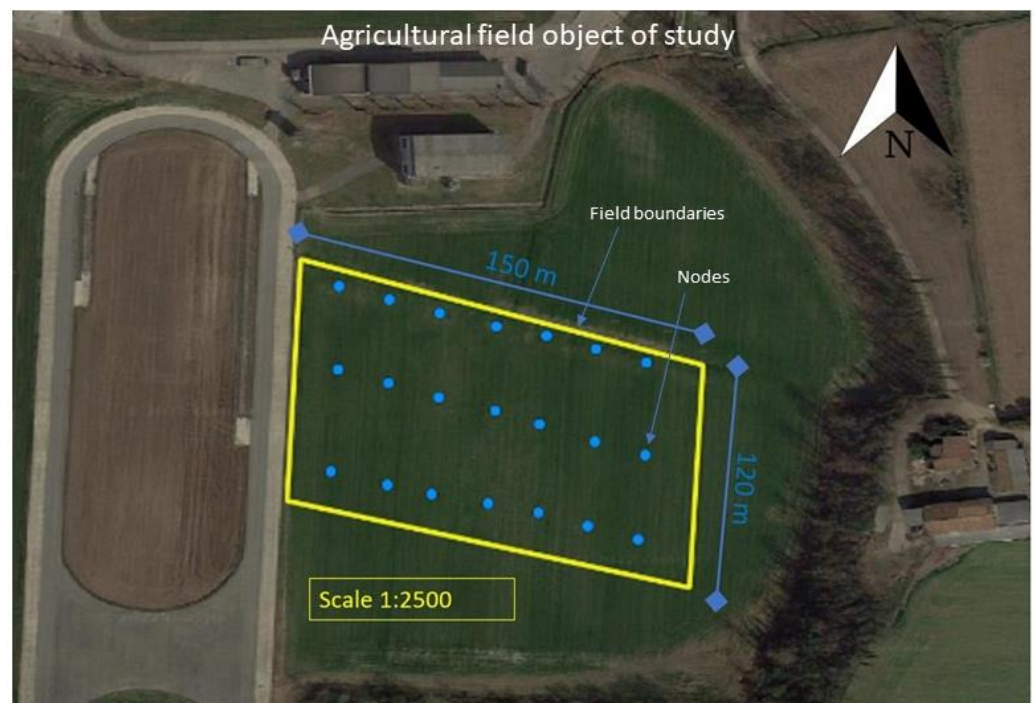


**Figure 1.** Experimental field of CREA-IT.

### 2.1. Proximal Monitoring—Geoelectric Survey

The soil was tested for electrical conductivity utilizing two methods. The first method involved the use of the Automatic Resistivity Profiler (A.R.P.; Geocarta SA, Paris, France). It is a mobile system consisting of three pairs of metal gear wheels. The first pair functions as

injection electrodes and the other 2 pairs function as receivers, which measure the electrical potential difference (Figure 2). The distance between each pair of receivers was calibrated to study 3 depths (0–50 cm, 0–100 cm, and 0–180 cm). The raw data was filtered using a 1D median filter and then interpolated to obtain a soil resistivity map ( $2 \times 2$  m pixels) for each layer studied.



**Figure 2.** Mobile system to measure the electrical potential difference.

The second method of geoelectric survey was performed by placing a network of 21 transmitting nodes in the ground according to a regular grid measuring  $20 \times 40$  m (Figure 1—blue points). Each node was composed of 2 capacitive soil moisture sensors, model SKU:SEN0193, placed respectively at 15 cm and 30 cm depth. The technology, unlike other sensors on the market, performs measurements through capacitive sensing. The operating voltage of the sensor is 3.3–5.5 VDC, the output Voltage is 0–3.0 VDC, and the operating current is 5 mA. The system is integrated into a DFRduino UNO hardware and an Arduino IDE V1.6.5 software. Each sensor was calibrated in the laboratory, checking the correspondence of the variations of the readings with soil samplings by studying soil moisture according to referring standard [25]. The readings were expressed in terms of spatial variation and not in absolute values to avoid eventual flaws or imperfections. The nodes are transmitted via a LoRa (Long Range) radio frequency to a receiving unit connected to a Wi-Fi network. Two of the nodes also had an air temperature and a humidity sensor (model DHT11 DF Robot). The data was acquired and transmitted with a time-frequency of 15 min. Before the geostatistical analysis, all the coordinates that were retrieved from the mapping tools and nodes were converted from geographic coordinates (World Geodetic System 84-WGS84) into Cartesian UTM coordinates using the “spTransform” function of the “rgdal” package [26]. All statistical processing followed the methodology indicated by Córdoba [27].

## 2.2. Remote Monitoring—Satellite Reading

Throughout the observation period, the maps of the spectrum bands available from two satellites (Sentinel A and B) were downloaded from the ESA website (European Space



Agency, [www.esa.int](http://www.esa.int), accessed on 1 September 2022.). In particular, the bands utilized were the B3 (560 nm), the B4 (675 nm), the B8 (842 nm) and B11 (1610 nm). These bands were necessary to obtain the MCARI2 (Modified Chlorophyll Absorption in Reflectance Index 2) and NDWI (Normalized difference water index) spectral indices, described in the following formulas:

$$MCARI2 = \frac{1.5[2.5(R_{842 \text{ nm}} - R_{675 \text{ nm}}) - 1.3(R_{842 \text{ nm}} - R_{560 \text{ nm}})]}{\sqrt{[2R_{842 \text{ nm}} + 1]^2 - [6(R_{842 \text{ nm}} - 5\sqrt{R_{675 \text{ nm}}} - 0.5)]}} \quad (1)$$

$$NDWI = \frac{R_{560 \text{ nm}} - R_{842 \text{ nm}}}{R_{560 \text{ nm}} + R_{842 \text{ nm}}} \quad (2)$$

The MCARI2 spectral index was chosen because it was considered suitable for the predictions of some biophysical parameters of plants [28–31], while the NDWI index was chosen because it is more correlated to the presence of water in the crop and uncultivated soil [32,33], but also because its correlation with soil fertility characteristics had been recently described and evaluated [34].

### 2.3. Monitoring of Meteorological Precipitation

The meteorological data were monitored through a local meteorological station located near the fields, which collected hourly data relating to the temperature and humidity of the air and millimeters of rain.

### 2.4. Dataset and Statistical Analysis

The dataset collected in the experimental fields during the observation period was composed of the following dependent variables:

- the measurements for each geographic soil coordinate of the electrical conductivity obtained from the ARP system;
- the difference in electrical conductivity detected by the surface sensors compared to those placed in the depth of the network of the transmitter nodes, with a frequency of 15 min;
- The spectral indices NDWI and MCARI2 are calculated by the Sentinel 2 source.

The independent variables of the experiment were the meteorological data (mm of rain) and the field conditions (crop present or not).

The methodology of data processing was dependent on the satellite information, both for resolution (20 m × 20 m) and dates of availability to be compared. During the whole observation period, 55 maps of the spectral bands of the two satellites were downloaded and observed. However, from these, only maps with no interference due to cloud densities were used. There is a list below of the dates when maps were sharp and implementable (Table 1).

From the available dates, the spectral indices MCARI2 and NDWI were calculated; the spectral bands utilized were the B3, the B4, and the B8 for MCARI2 and the bands B3 and B11 for the NDWI. The B3, B4, and B8 bands are available with a resolution of 10 m × 10 m, while the B11 band relating to the short-wave infrared (SWIR) has a resolution of 20 m × 20 m.

Therefore, for the source of information coming from the sensor network, a data filter was carried out by selecting the dates and times corresponding to the passage of the satellites. The differences in conductivity between the sensor placed on the soil surface and that placed 0.15 m deeper were calculated.

For the geoelectric source, spatial vectors were prepared and subjected to clustering for the determination of homogeneous zones. From these zones, soil samples were taken in order to establish their composition in sand, silt and clay. Subsequently, a vector with the information obtained from the sampling point was extracted. The flow chart depicted in

Figure 3 shows that information from spatial raster coming from the satellites was extracted as well and corresponded to the coordinates of the ground sensors.

**Table 1.** Dates of availability of information used for this study.

Date	Condition	mm Rain (Last 5 Days Cumulative)
25 July 2020	corn	66.50
30 July 2020	corn	42.80
9 August 2020	corn	40.00
14 August 2020	corn	0.00
19 August 2020	corn	40.00
13 September 2020	corn	0.00
19 September 2020	corn	0.00
17 November 2020	soil	4.30
22 November 2020	soil	0.00
27 December 2020	soil	42.40
16 January 2021	triticale	0.00
15 February 2021	triticale	16.50
25 February 2021	triticale	0.00
2 March 2021	triticale	0.00
7 March 2021	triticale	0.00
17 March 2021	triticale	0.00
22 March 2021	triticale	0.00

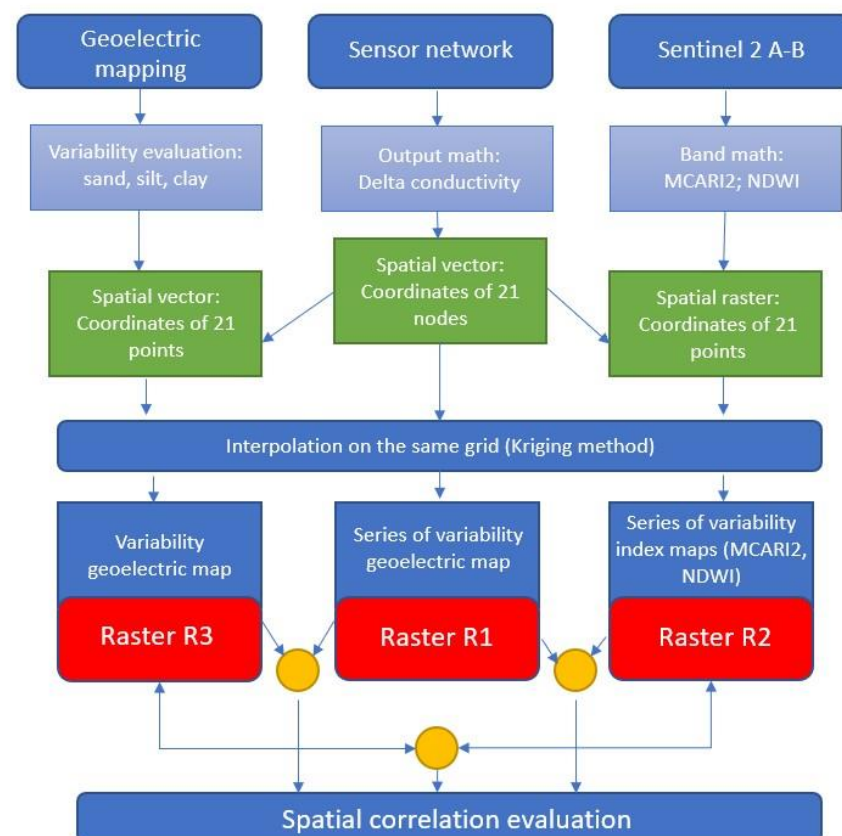


**Figure 3.** Flow diagram of the correlation study.

The data were subjected to geostatistical analysis using the “R” statistical software. The values coming from the three sources, with the same coordinates for construction, were interpolated with the kriging method through the krige function of the *gstat* package of R, using a regular grid of  $5\text{ m} \times 5\text{ m}$  points in the quadrilateral defined by the area observed by the sensor network, to observe its distribution in space.

Therefore, 17 rasters interpolated from the values came from the sensor network (R1); 17 rasters interpolated for satellite information (R2), and 1 raster from the geoelectric reading (R3) were obtained.

To verify the correlation between the corresponding rasters of the same day (from satellite and from the sensor network) and between these and the 1 relating to the geoelectric reading, the analysis of correlation was applied based on the moving window of Dutilleul [35].

The analysis of variance (ANOVA) was applied to the values of the correlations obtained for each available date, considering as independent variables the conditions of the field based on the coverage (triticale, bare soil, and maize) and based on the water conditions. This took into consideration if the soil had received in the previous 5 days a quantity of water greater than 40 mm, in the form of both rain and irrigation.

### 3. Results

The range of soil water content monitored with soil sensors (average of 21 nodes) was reported for the dates of satellite data availability (Figure 4). The values are represented with the independent variables considered for the experiment, i.e., meteorological data (mm of rain in the green square) and the field conditions (corn, soil, and triticale). Higher variability was noted for corn on 25 July 2020, for soil on 27 December 2020, and for triticale on 2 January 2021 (Figure 5).

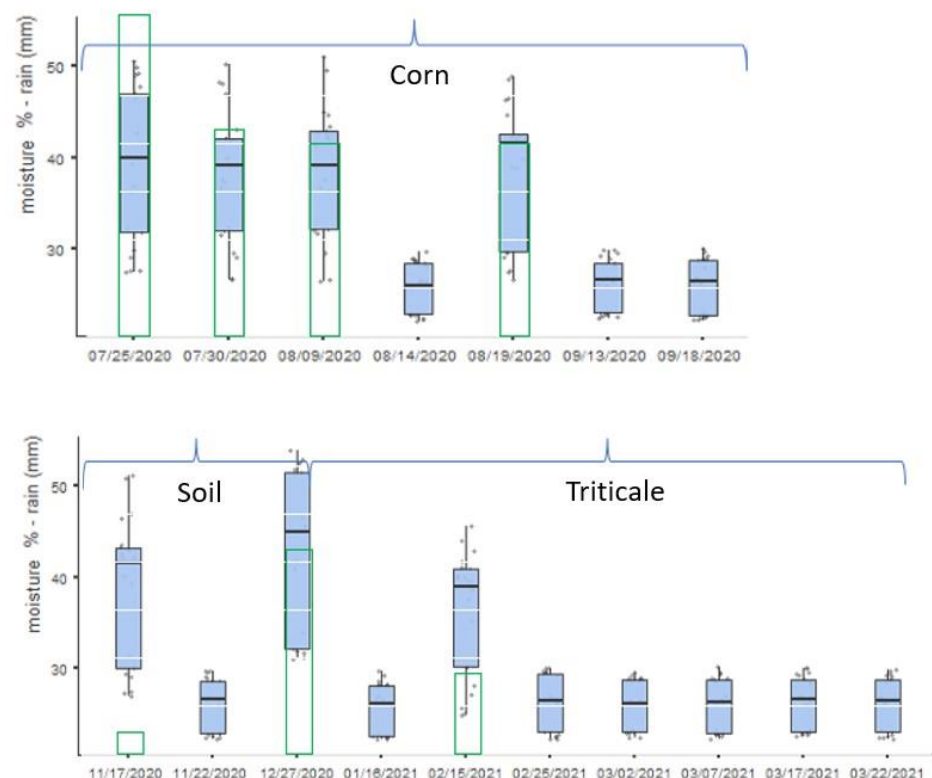


**Figure 4.** Distribution of soil water content (%) and precipitation (mm, green line box) in the period of observation.

#### 3.1. Comparison between Sensor Grid Maps (R1) and Corresponding Satellite Maps (R2)

Using the MCARI2 index (Figure 6), greater correlation values were identified when the soil was not cultivated (correlation values close to 1) and when the corn was cultivated (correlations close to  $-1$ ). The use of the NDWI index has the opposite behavior, with many values close to 1 in the corn cultivation period and  $-1$  in the period in which the soil was without the crop. These results highlight that the comparison between grid and satellite maps delivers high correlation values during corn cultivation, with a negative direction for

MCARI2 and a positive one for NDWI. During the cultivation of triticale, the correlation values were very variable, and this did not define any trends.

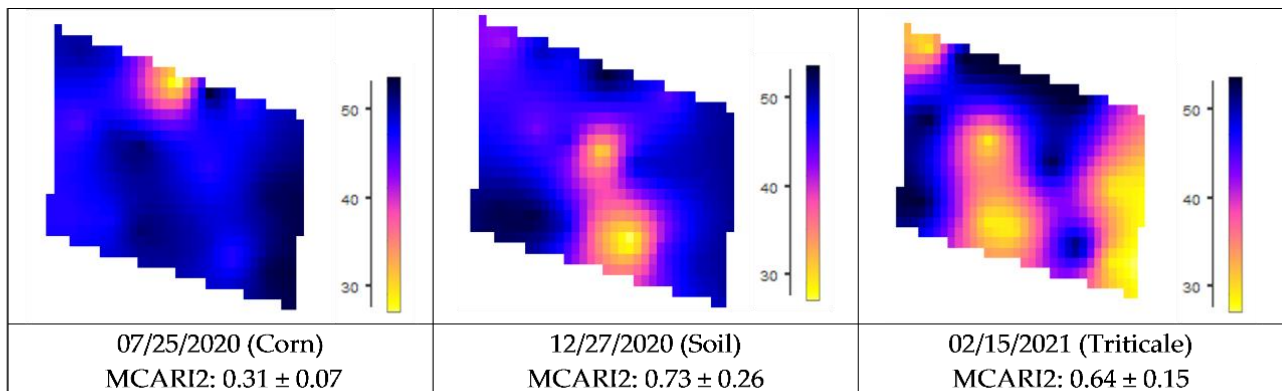


**Figure 5.** Example of soil water content (%) distribution map for three representative dates with average and standard deviation of MCARI2 index.

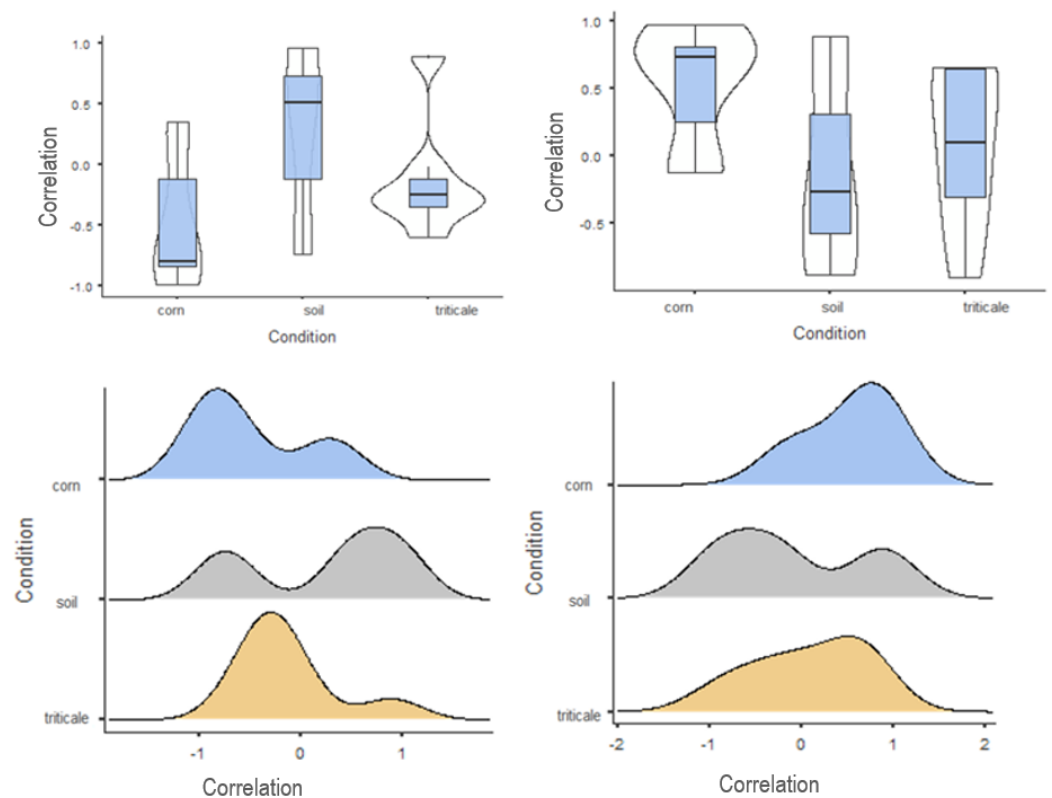


**Figure 6.** In the left column is the distribution of correlation values between the maps produced with the sensors and with the MCARI2 spectral index; in the right column is the distribution of correlation values between the maps produced with the sensors and with the NDWI spectral index.

### 3.2. Comparison between Sensor Grid Maps (R1) and Corresponding Geoelectric Maps (R3)

In the period of corn cultivation (25/07/2020–18/09/2020), correlation values of different intensities from  $-1$  to  $+1$  were identified with a widespread and homogeneous distribution of all values (Figure 7). In the period in which the soil was not cultivated, larger correlations were detected at  $-0.40$ , while in the period in which the triticale crop was present, correlation densities were closer to  $-1$ .



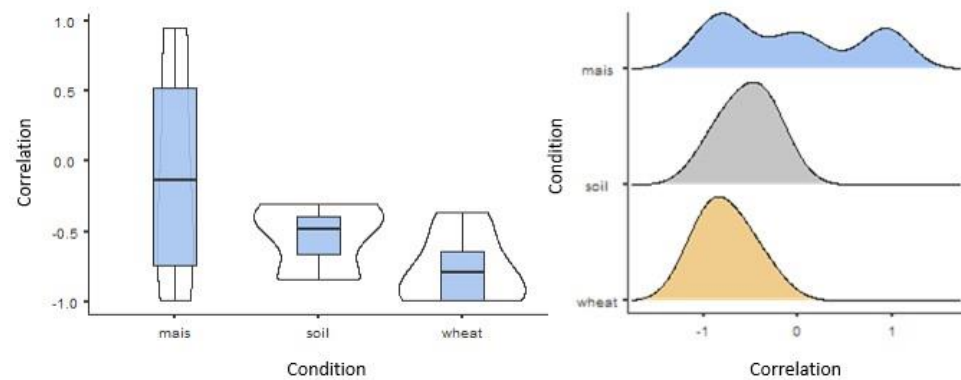


**Figure 7.** Distribution of the correlation values between maps produced with sensors and with the geoelectric method.

Therefore, results of the comparison between sensor grid maps and geoelectric maps demonstrate a scarce correlation of the system during corn cropping, while there was a higher correlation for both uncultivated soil and triticale cropping period with denser values close to  $-1$ .

### 3.3. Comparison between Geoelectric Maps (R3) and Corresponding Satellite Maps (R2)

The observation of the MCARI2 index (Figure 8) during the cultivation of corn shows a very homogeneous distribution of all correlation values, oscillating from  $-1$  to  $+1$  but also assuming values around 0.

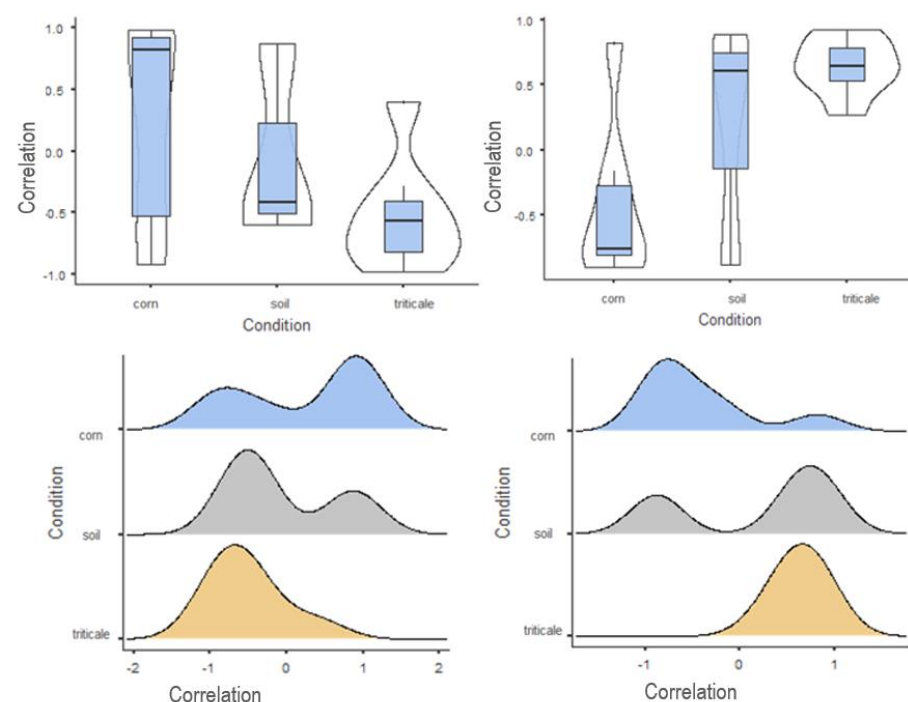


**Figure 8.** In the left column is the distribution of correlation values between the maps produced with the geoelectric method and with the MCARI2 spectral index. In the left column is the distribution of correlation values between the maps produced with the geoelectric method and with the NDWI spectral index.

In the condition of uncultivated soil, there are very few correlations close to 0, with higher densities of correlations close to 0.90 and  $-0.60$ . In the period of triticale cultivation, the correlations are mainly concentrated towards the value of  $-1$ . Regarding the NDWI index, in the period of corn cultivation, greater densities of correlations were identified at

−1 while presenting some correlations close to +1. In the period of uncultivated soil, the values appear to be homogeneously distributed between −1 and +1. On the other hand, dense values of correlations were identified in the triticale growing period with values close to +0.80.

Summarizing, the results showed that in the period in which the summer crop (corn) was present, the correlation between the sensor grid and the satellite maps was greater. In the period when the soil was not cultivated, the correlation between the sensor grid and the mapping with the ARP method was greater. Finally, in the period in which triticale was grown, the correlations between the ARP method, satellite maps, and the sensor grid were greater.

The analysis of variance (ANOVA) showed significance ( $p$ -value < 0.001) in the comparison between sensors and satellite maps (R1-R2) for both spectral indices and for the corn condition; between sensors and ARP (R1-R3) the condition of soil and triticale were similar but different compared to corn (Table 2). Finally, the comparison between ARP and satellite maps (R3-R2) showed statistically significant differences in both indices for the triticale condition. All comparisons, except for R1-R2 (MCARI2 used), showed statistical significance in case of rainy events greater than 40 mm, which occurred in the previous five days, also showing first-order interaction factors with this condition. This indicates that the results are influenced by the presence of water in the soil.

**Table 2.** Significance of the soil condition and soil moisture in relation to the correlations between the survey methods.

	Condition (Corn, Soil, Triticale)	Moisture (>40 mm)	Interaction Condition-Moiture
R1-R2 (MCARI2)	*** (corn)	n.s.	***
R1-R2 (NDWI)	*** (corn)	***	***
R1-R3	*** (soil, triticale)	***	***
R3-R2 (MCARI2)	*** (triticale)	***	***
R3-R2 (NDWI)	*** (triticale)	***	***

\*\*\* corresponds to  $p$ -value < 0.001.

#### 4. Discussion

The study showed that the three sources of information utilized have contributed to the representation of the soil moisture in the determined conditions. On the other hand, considering each source singularly, some limitations have been noted, especially in the case of different soil conditions and cultivations type (triticale, corn, uncultivated soil). The analysis of the correlation maps displayed interesting results that may lead to identifying “exclusivity” or “complementarity” between the methods. For exclusivity, it can be intended that one system (e.g., satellite system) may replace another (e.g., soil sensor) because of high correlations. However, for complementarity, we intend that one method can be functionally similar to another for the goal of defining a precision irrigation schedule. This complementarity was observed in the conditions of minor correlation between the reading methods. For instance, the maps obtained from the ground sensors (R1) showed less correlation with the satellite maps (R2) when the soil was cultivated with triticale, with an average correlation of −0.02 for the MCARI2 index and of 0.1 for the ‘NDWI index. Therefore, in the period in which the triticale was cultivated, the satellite indices did not allow us to obtain maps corresponding to the proximal readings. This was probably because of the meteorological trend, which showed a significant influence on the values of correlation. Instead, the satellite information (R2) correlate with those of soil sensor (R1) during corn cultivation, meaning that the satellite, in this case, can substitute the information of soil sensors.

The same consideration applies to both geoelectric methods (R1 and R3) and between the MCARI2 satellite index and ARP (R2 and R3). The two geoelectric methods showed an average correlation in the period of uncultivated soil (−0.45) and in the period of corn

cultivation ( $-0.2$ ). This can be attributable to the fact that reading with ARP (R3) was performed only once, while the readings with the soil sensors (R1) were performed at a high frequency, detecting variations over time. On the other hand, the same was also observed between the maps processed through the MCARI2 satellite index and the map obtained with the ARP, showing a very low correlation, lower than  $-0.4$ , in the condition of uncultivated soil.

Previous studies have observed correlations between soil moisture and electromagnetic observations in the visible-near infrared [36,37], in the thermal infrared [38,39] and in microwaves [40–42].

Based on these correlations, Ma et al. [39] have considered the opportunity to detect and localize the variability of soil moisture. Additionally, the study conducted by Balenzano et al. [43] explored the need to integrate soil surface humidity indexes and vegetation indexes to plan irrigation events during the entire vegetative season.

However, despite the numerous studies performed, the extreme soil variability and the different field conditions may limit the applicability of the use of satellite indexes for this purpose.

The most interesting aspect of this study is the correlation and complementarity between the sensor network and the satellite indexes. This is because sensor networks can be considered the most reliable and repeatable measurements, while satellite indexes are the most affordable. Potential future approaches may look for complementarity between satellite indexes with a significantly reduced number of sensors. Reducing the number of sensors may decrease the initial investment cost for farmers, but at the same time, farmers may rely on satellites for scheduling precision irrigation interventions.

## 5. Conclusions

The aim of this study was to evaluate the correlation between three soil water content investigation techniques in an effort to understand if satellite data obtained from remote sensing has a high potential for use in the management of water resources and in precision irrigation, as well as no-vegetation conditions. The results showed that indexes utilized from satellite data correlate in different cases with proximal sensing methods. Even if the method cannot be considered fully satisfactory, the high correlation between the MCARI2 and the in-field sensor network suggests possible applications in the condition of bare soils. This opens the opportunity to monitor soils after sowing to guarantee the success of the seed emergence. To fully exploit the potential of this approach, its association with proximal investigation methods is still recommended. These aspects will be investigated in future studies. In view of using digital systems to make living conditions simpler and affordable for the population, this paper has contributed towards exploring satellite technology to facilitate the process of planning precision irrigation and to reduce the costs of investment in tools and equipment for future farming generations.

**Author Contributions:** Conceptualization, E.R., S.B., C.B., R.P. and A.S.; Data curation, E.R.; Formal analysis, E.R.; Methodology, S.B.; Supervision, C.B. and A.S.; Validation, R.P.; Writing—original draft, E.R., S.B. and A.S.; Writing—review & editing, S.B., C.B., R.P. and A.S. All authors have read and agreed to the published version of the manuscript.

**Funding:** This work was supported by the Italian Minister of Agriculture, Food Sovereignty and Forests (MASAF) as part of the project “AGRIDIGIT” subproject “AGROFILIERE” DM n. 36503 of 20/12/2018.

**Data Availability Statement:** Ethical review and approval were waived for this study because they were not applicable.

**Acknowledgments:** The authors wish to thank Elia Premoli, Alex Filisetti, and Ivan Carminati for their assistance in performing field operations and for their professionalism and availability.

**Conflicts of Interest:** The authors declare no conflict of interest.

## References

1. Fioravanti, G.; Frascchetti, P.; Lena, F.; Perconti, W.; Piervitali, E.; Pavan, V. Gli Indicatori del Clima in Italia nel 2020. ISPRA: Rome, Italy, 2020. Available online: <https://www.isprambiente.gov.it/it/pubblicazioni/stato-dellambiente/gli-indicatori-del-clima-in-italia-nel-2020-anno-xvi> (accessed on 1 September 2022).
2. National Centers for Environmental Information (NOAA). State of the Climate: Monthly Global Climate Report for Annual 2020. 2021. Available online: <https://www.ncei.noaa.gov/access/monitoring/monthly-report/global/202013> (accessed on 1 September 2022).
3. ISTAT. Available online: <https://www.istat.it/it/archivio/5679> (accessed on 10 July 2022).
4. ISTAT. Available online: <https://www.istat.it/it/archivio/202875> (accessed on 10 July 2022).
5. OECD. *Water Risk Hotspots for Agriculture, OECD Studies on Water*; OECD Publishing: Paris, France, 2017. [CrossRef]
6. Bjorneberg, D.L. IRRIGATION Methods. In *Reference Module in Earth Systems and Environmental Sciences*; Elsevier: Amsterdam, The Netherlands, 2013. [CrossRef]
7. Uddin, M.J. Measurements of Evaporation during Sprinkler Irrigation. Ph.D. Thesis, UNISQ—Historic—Faculty of Engineering and Surveying, Toowoomba, Australia, 2012. Available online: <https://eprints.usq.edu.au/23481/> (accessed on 1 September 2022).
8. Afrin, M. Evaporation loss during sprinkler irrigation. *Bangladesh J. Scient. Res.* **2010**, *23*, 81–90.
9. Smith, R.J.; Baillie, J.N.; Mc Carthy, A.C.; Raine, S.R.; Baillie, C.P. Review of Precision Irrigation Technologies and Their Application. Australia (2010) or Adeyemi, O.; Grove, I.; Peets, S.; Norton, T. Advanced Monitoring and Management Systems for Improving Sustainability in Precision Irrigation. *Sustainability* **2017**, *9*, 353.
10. Millán, S.; Casadesús, J.; Campillo, C.; Moñino, M.J.; Prieto, M.H. Using Soil Moisture Sensors for Automated Irrigation Scheduling in a Plum Crop. *Water* **2019**, *11*, 2061. [CrossRef]
11. Maughan, T.; Allen, L.N.; Drost, D. Soil Moisture Measurement and Sensors for Irrigation Management. In *Extension and Agriculture*; Utah State University: Logan, UT, USA, 2015; Available online: [https://digitalcommons.usu.edu/cgi/viewcontent.cgi?article=1777&context=extension\\_curall](https://digitalcommons.usu.edu/cgi/viewcontent.cgi?article=1777&context=extension_curall) (accessed on 5 September 2022).
12. Ruixiu, S. Irrigation Scheduling Using Soil Moisture Sensors. *J. Agric. Sci.* **2017**, *10*, 1.
13. Pramanik, M.; Khanna, M.; Singh, M.; Singh, D.K.; Sudhishri, S.; Bhatia, A.; Ranjan, R. Automation of soil moisture sensor-based basin irrigation system. *Smart Agr. Technol.* **2022**, *2*, 100032. [CrossRef]
14. Aguilar, J.; Rogers, D.; Kisekka, I. Irrigation Scheduling Based on Soil Moisture Sensors and Evapotranspiration, Kansas. *Agric. Exp. Stn. Res. Rep.* **2015**, *1*, 5. [CrossRef]
15. O'Shaughnessy, S.A.; Evett, S.R.; Colaizzi, P.D.; Andrade, M.A.; Marek, T.H.; Heeren, D.M.; Lamm, F.R.; LaRue, J.L. Identifying Advantages and Disadvantages of Variable Rate Irrigation—An Updated Review. *Biol. Syst. Eng.* **2019**, *35*, 837–852. [CrossRef]
16. Li, Y.; Wang, Y.; Li, B.; Wu, S. Super-Resolution of Remote Sensing Images for  $\times 4$  Resolution without Reference Images. *Electronics* **2022**, *11*, 3474. [CrossRef]
17. Ou, Z.; Qu, K.; Wang, Y.; Zhou, J. Estimating Sound Speed Profile by Combining Satellite Data with In Situ Sea Surface Observations. *Electronics* **2022**, *11*, 3271. [CrossRef]
18. Ivanda, A.; Šerić, L.; Bugarić, M.; Braović, M. Mapping Chlorophyll-a Concentrations in the Kaštela Bay and Brač Channel Using Ridge Regression and Sentinel-2 Satellite Images. *Electronics* **2021**, *10*, 3004. [CrossRef]
19. Massari, C.; Modanesi, S.; Dari, J.; Gruber, A.; De Lannoy, G.J.; Giroto, M.; Quintana-Seguí, P.; Le Page, M.; Jarlan, L.; Zribi, M. A Review of Irrigation Information Retrievals from Space and Their Utility for Users. *Remote Sens.* **2021**, *13*, 4112. [CrossRef]
20. De Lara, A.; Longchamps, L.; Khosla, R. Soil Water Content and High-Resolution Imagery for Precision Irrigation: Maize Yield. *Agronomy* **2019**, *9*, 174. [CrossRef]
21. Ihuoma, S.O.; Madramootoo, C.A.; Kalacska, M. Integration of satellite imagery and in situ soil moisture data for estimating irrigation water requirements. *Intern. J. Appl. Earth Observ. Geoinform.* **2021**, *102*, 102396. [CrossRef]
22. Tang, J.; Busso, C.A.; Jiang, D.; Wang, Y.; Wu, D.; Musa, A.; Miao, R.; Miao, C. Seed Burial Depth and Soil Water Content Affect Seedling Emergence and Growth of *Ulmus pumila* var. *sabulosa* in the Horqin Sandy Land. *Sustainability* **2016**, *8*, 68. [CrossRef]
23. Hou, D.; Bi, J.; Ma, L.; Zhang, K.; Li, D.; Rehmani, M.I.A.; Tan, J.; Bi, Q.; Wei, Y.; Liu, G.; et al. Effects of Soil Moisture Content on Germination and Physiological Characteristics of Rice Seeds with Different Specific Gravity. *Agronomy* **2022**, *12*, 500. [CrossRef]
24. IUSS Working Group WRB. *World Reference Base for Soil Resources*; World Soil Resources Reports; IUSS Working Group WRB: Österreich, Austria, 2015; No. 106.
25. ISO 11461:2001. Soil Quality—Determination of Soil Water Content as a Volume Fraction Using Coring Sleeves—Gravimetric Method. ISO: Geneva, Switzerland, 2001.
26. Bivand, R.; Keitt, T.; Rowlingson, B. Bindings for the Geospatial Data Abstraction Library. R Package Version 0.8-16. 2008. Available online: <http://CRAN.R-project.org/package=sp> (accessed on 1 November 2016).
27. Córdoba, M.A.; Bruno, C.I.; Costa, J.L.; Peralta, N.R.; Balzarini, M.G. Protocol for multivariate homogeneous zone delineation in precision agriculture. *Biosyst. Eng.* **2016**, *143*, 95–107. [CrossRef]
28. Leolini, L.; Moriondo, M.; Rossi, R.; Bellini, E.; Brilli, L.; López-Bernal, Á.; Santos, J.A.; Fraga, H.; Bindi, M.; Dibari, C.; et al. Use of Sentinel-2 Derived Vegetation Indices for Estimating fPAR in Olive Groves. *Agronomy* **2022**, *12*, 1540. [CrossRef]
29. Romano, E.; Bergonzoli, S.; Pecorella, I.; Bisaglia, C.; De Vita, P. Methodology for the Definition of Durum Wheat Yield Homogeneous Zones by Using Satellite Spectral Indices. *Remote Sens.* **2021**, *13*, 2036. [CrossRef]

30. Wu, C.; Niu, Z.; Tang, Q.; Huang, W. Estimating chlorophyll content from hyperspectral vegetation indices: Modeling and validation. *Agric. For. Meteorol.* **2008**, *148*, 1230–1241. [[CrossRef](#)]
31. Haboudane, D.; Miller, J.R.; Pattey, E.; Zarco-Tejada, P.J.; Strachan, I.B. Hyperspectral vegetation indices and novel algorithms for predicting green LAI of crop canopies: Modeling and validation in the context of precision agriculture. *Remote Sens. Environ.* **2004**, *90*, 337–352. [[CrossRef](#)]
32. Balajee, J.; Saleem Durai, M.A. Drought Prediction and Analysis of Water level based on satellite images Using Deep Convolutional Neural Network. *Int. J. Speech Technol.* **2022**, *25*, 615–623. [[CrossRef](#)]
33. Onáčillová, K.; Gallay, M.; Paluba, D.; Péliová, A.; Tokarčík, O.; Laubertová, D. Combining Landsat 8 and Sentinel-2 Data in Google Earth Engine to Derive Higher Resolution Land Surface Temperature Maps in Urban Environment. *Remote Sens.* **2022**, *14*, 4076. [[CrossRef](#)]
34. Mazur, P.; Gozdowski, D.; Wójcik-Gront, E. Soil Electrical Conductivity and Satellite-Derived Vegetation Indices for Evaluation of Phosphorus, Potassium and Magnesium Content, pH, and Delineation of Within-Field Management Zones. *Agriculture* **2022**, *12*, 883. [[CrossRef](#)]
35. Dutilleul, P. Modifying the t test for assessing the correlation between two spatial processes. *Biometrics* **1993**, *49*, 305–314. [[CrossRef](#)]
36. Wang, Y.; Peng, J.; Song, X.; Leng, P.; Ludwig, R.; Loew, A. Surface soil moisture retrieval using optical/thermal infrared remote sensing data. *IEEE Trans. Geosci. Remote Sens.* **2018**, *56*, 5433–5442. [[CrossRef](#)]
37. Kang, J.; Jin, R.; Li, X.; Ma, C.F.; Qin, J.; Zhang, Y. High spatio-temporal resolution mapping of soil moisture by integrating wireless sensor network observations and MODIS apparent thermal inertia in the Babao River Basin, China. *Remote Sens. Environ.* **2017**, *191*, 232–245. [[CrossRef](#)]
38. Leng, P.; Song, X.N.; Duan, S.B.; Li, Z.L. Generation of continuous surface soil moisture dataset using combined optical and thermal infrared images. *Hydrol. Process* **2017**, *31*, 1398–1407. [[CrossRef](#)]
39. Ma, C.F.; Wang, W.Z.; Han, X.J.; Li, X. Soil moisture retrieval in the heihe river basin based on the real thermal inertia method. *IEEE J. Sel. Top. Appl. Earth Obs. Remote Sens.* **2013**, *6*, 1460–1467. [[CrossRef](#)]
40. Kerr, Y.H.; Waldteufel, P.; Wigneron, J.P.; Martinuzzi, J.; Font, J.; Berger, M. Soil moisture retrieval from space: The soil moisture and ocean salinity (SMOS) mission. *IEEE Trans. Geosci. Remote Sens.* **2001**, *39*, 1729–1735. [[CrossRef](#)]
41. Wagner, W.; Lemoine, G.; Rott, H. A Method for estimating soil moisture from ERS scatterometer and soil data. *Remote Sens. Environ.* **1999**, *70*, 191–207.
42. Zho, T.; Hu, L.; Shi, J.; Lü, H.; Li, S.; Fan, D.; Wang, P.; Geng, D.; Kang, C.S.; Zhang, Z. Soil moisture retrievals using L-band radiometry from variable angular ground-based and airborne observations. *Remote Sens. Environ.* **2020**, *248*, 111958. [[CrossRef](#)]
43. Balenzano, A.; Satalino, G.; Lovergine, F.P.; D’Addabbo, A.; Palmisano, D.; Grassi, R.; Ozalp, O.; Mattia, F.; Nafria, G.D.; Paredes, G.V. Sentinel-1 and Sentinel-2 Data to Detect Irrigation Events: Rianza Irrigation District (Spain) Case Study. *Water* **2022**, *14*, 3046. [[CrossRef](#)]

**Disclaimer/Publisher’s Note:** The statements, opinions and data contained in all publications are solely those of the individual author(s) and contributor(s) and not of MDPI and/or the editor(s). MDPI and/or the editor(s) disclaim responsibility for any injury to people or property resulting from any ideas, methods, instructions or products referred to in the content.